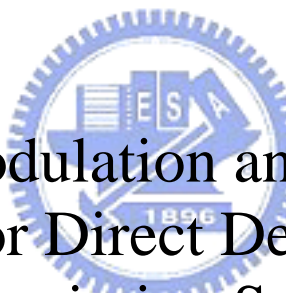


國立交通大學
光電工程研究所
博士論文

先進光調變與多工技術在直接偵測光傳
輸系統上的性能評估與分析



Advanced Modulation and Multiplexing
Techniques for Direct Detection Optical
Transmission Systems

研究生：彭煒仁

指導教授：祁 姓 教授

中華民國九十七年六月

先進光調變與多工技術在直接偵測光傳
輸系統上的性能評估與分析

Advanced Modulation and Multiplexing
Techniques for Direct Detection Optical
Transmission Systems

研究生：彭煒仁 Student：Wei-Ren Peng
指導教授：祁 甦 Advisor：Sien Chi



國立交通大學 電機學院
光電工程研究所
博士論文

A Dissertation
Submitted in Partial Fulfillment of the Requirements
for the Degree of Doctor of Philosophy in
The Institute of Electro-Optical Engineering
College of Electrical and Computer Engineering
National Chiao Tung University
Hsin-Chu, Taiwan, R.O.C.

中華民國九十七年六月

先進光調變與多工技術在直接偵測光傳輸

系統上的性能評估與分析

研究生：彭煒仁

指導教授：祁 銓

國立交通大學 電機學院

光電工程研究所

摘要

在本論文中我們將簡介數種已提之先進光調變格式以及光多工技術，其工作原理以及目前所遇到的議題將一併於論文中予以討論以及部分解決。其中光多工技術包含光正交頻分多工 (OFDM) 以及光碼分多工 (OCDMA) 兩種技術，而光調變格式主要是高頻譜效能(>1 bit/symbol) 之格式包含多階相位或多階振幅調變格式。

針對直接偵測 OFDM 下我們提出射頻輔助正交分頻多工(RF-tone assisted OFDM)以及廣義虛擬單邊帶正交頻分多工(Generalized Virtual SSB-OFDM)等兩種技術。此技術置放一射頻次載波於信號頻帶邊緣作為遠端直接偵測參考信號之用。使用我們的技術後，和同性質的直接升頻(direct up-conversion) 調變器相比，可節省一半數位轉類比器(DAC) 的取樣速度，而其 DAC 有限的取樣速度在高容量 (≥ 10 Gbps) 的光通訊傳輸下目前乃是主要瓶頸。此外，我們成功地傳輸 10 Gbps OFDM 訊號經過 1600 km 的標準單模光纖後僅 3 dB 的損傷，驗證此技術在未來光通訊的應用潛力。

於光調變格式中，我們實驗以及理論驗證其使用簡易、低廉的單顆光調變器產生數種複雜傳輸訊號的可能性。這在未來講求低價格，高效能的光通訊網路上是一大躍進。除此之外我們更進而分析數種不同調變格式的性能理論上限：量子限制 (quantum limit)。此一限制給出最佳性能指標以簡化工程應用上所能達成的最佳性能。

最後我們研究光碼分多工技術在局部網路(LAN)上的應用。我們使用費比布洛自注入雷射以及光纖光柵串列提出廉價光碼分多工光源。藉著針對每一個光柵施以溫度或應

力的控制我們可以改變所要傳送地點的用戶碼。接著提出交叉頻率分組方式以降低在多用戶光碼分多工系統下所遭遇到的多重存取干擾。最後，我們首次實驗驗證多載波碼分多工系統於光接取網路上的應用可能。



Advanced Modulation and Multiplexing Techniques for Direct Detection Optical Transmission Systems

Student: Wei-Ren Peng

Advisor: Sien Chi

Institute of Electro-Optical Engineering
College of Electrical and Computer Engineering
National Chiao Tung University

ABSTRACT

In this dissertation, we review and propose several new approaches for orthogonal frequency division multiplexing (OFDM), advanced modulation formats, and code division multiplexing (OCDM) techniques in optical transmission systems.

For OFDM, we propose an RF-tone assisted OFDM and virtual single-sideband OFDM (VSSB-OFDM) systems for direct detected optical transmission. With an RF tone inserted at the edge of the signal band, the sensitivity and CD tolerance are both improved compared to the previous power modulated SSB-OFDM. Besides, our approach also relaxes the bandwidth requirement for digital to analog converter (DAC) which would be very critical in a high speed transmission with a data rate of ≥ 10 Gbps. In addition, we firstly propose a 2x2 matrix equalization technique to jointly compensate the distortions resulted from both the transmission and the imbalances of the optical modulator. Moreover, we successfully transmit a 4-QAM, 10-Gbps signal through 1600 km uncompensated standard single mode fiber (SSMF) with only ~ 3 dB penalty, which is smaller than any other proposed direct-detected transmission systems.

For advanced modulation formats, we numerically evaluate and experimentally demonstrate the generation of complex modulation formats by using one dual-drive

Mach-Zehnder modulator (DD-MZM). We also analyze the performance bound, i.e. quantum limit, of 4ASK format. We further propose a phase modulated 4ASK (PM4ASK) format which shows a better CD, PMD and filtering tolerances compared to conventional 4ASK format.

For CDMA, we propose a simple and cost-effective fast frequency hopping CDMA (FFH-CDMA) light source which uses a self-injected Fabry Perot laser and one string of fiber Bragg grating array (FBGA). By tuning the stress of each individual grating, we can encode the transmitted data by the destination codeword. Aimed to eliminate the inherent multiple access interference (MAI) in optical FFH-CDMA, we propose a frequency-interleaved multi-group approach which fully uses the frequency gap between the gratings to reduce the spectrum overlapping among different users, and design the new codeword searched by computers which is suitable for this proposed technique. Finally we verify this technique by some simulation results.



誌 謝

(Acknowledgements)

感謝祁姓 (Dr. Sien Chi) 老師這段期間在學業上細心地指導與教誨，也讓我學習到許多做人處事之道。同時也感謝南加州大學電機系教授 Dr. Alan E. Willner 耐心地教導，使得在研究上所遇到的瓶頸，總是能迎刃而解。

此外，也感謝實驗室合作教授交大光電所陳智弘 (Dr. Jyehong Chen)以及清大電通所馮開明 (Dr. Kai-Ming Feng) 的長期幫忙和指點。特別感謝台灣交通大學: 彭朋群 (Peng-Chun Peng)，錢鴻章(Hung-Chang Chien)，林俊廷(Chun-Ting Lin)以及黃明芳 (Ming-Fang Huang)博士；以及南加州大學: 章波(Bo Zhang)，張林(Lin Zhang)，武曉霞 (Xiaoxia Wu)以及台灣同胞楊振源(Jeng-Yuan Yang)同學等同儕的相互勉勵及協助，使研究之路得以順利且充滿樂趣。

最後感謝我最摯愛的父母、家人，謝謝你們的關懷與一路扶持。



Contents

Chinese Abstract.....	I
English Abstract.....	III
Acknowledgement.....	V
Contents.....	VI
List of Figures.....	XII
List of Table.....	XIX
List of Acronyms.....	XX

Chapter 1

Introduction

1.1 Background.....	1
1.2 Motivation.....	4
1.3 Organization of the Dissertation.....	5
References.....	7



Chapter 2

Overviews of Optical Modulation and Multiplexing Techniques

2.1 Introduction.....	8
2.2 Optical Orthogonal Frequency Division Multiplexing (OFDM)	
2.2.1 Coherent Detection.....	9
2.2.2 Direct Detection.....	11
2.3 Advanced Modulation Formats	
2.3.1 Differential Phase Shift Keying (DPSK).....	13
2.3.2 Differential Quadrature Phase Shift Keying (DQPSK).....	13

2.3.3	Other Four-Level Modulation Formats.....	14
2.3.4	Analysis Tools for Modulation Formats.....	15
2.4	Optical Code division Multiplexing (OCDM)	
2.4.1	Direct-Sequence CDMA (DS-CDMA).....	16
2.4.2	Fast Frequency Hopping CDMA (FFH-CDMA).....	17
2.4.3	Spectra-Encoded CDMA (SE-CDMA).....	17
	References.....	18

Chapter 3

Optical Orthogonal Frequency Division Multiplexing

3.1	Introduction.....	28
3.2	RF tone Assisted Optical OFDM Systems	
3.2.1	Experimental Demonstration of a Coherently Modulated and Directly Detected Optical OFDM System Using an RF-Tone Insertion	
3.2.1.1	Introduction.....	29
3.2.1.2	Concept.....	30
3.2.1.3	Equalization.....	31
3.2.1.4	Experimental Setup and Results.....	32
3.2.1.5	Summary.....	34
3.2.2	Experimental Demonstration of Compensating the I/Q Imbalance and Bias Deviation of the Mach-Zehnder Modulator for an RF Tone Assisted Optical OFDM System	
3.2.2.1	Introduction.....	34
3.2.2.2	Effects of I/Q Imbalance and Bias Deviation.....	35
3.2.2.3	Compensation for I/Q Imbalance and Bias Deviation.....	36
3.2.2.4	Experimental Setup and Results.....	36

3.2.2.5	Summary.....	37
3.2.3	Tunable Optical Wavelength Conversion of a 10 Gb/s OFDM Data Signal Using a Periodically-Poled Lithium Niobate Waveguide	
3.2.3.1	Introduction.....	38
3.2.3.2	Concept.....	39
3.2.3.3	Experimental Results.....	39
3.2.3.4	Summary.....	41
3.2.4	Theoretical Investigations	
3.2.4.1	The Optimum Carrier to Signal Power Ratio (CSPR).....	41
3.2.4.2	Bit Error Rate Calculation for a Single Sideband OFDM Signal with Direct Detection optically Pre-amplified Receivers.....	42
3.3	Virtual Single Sideband OFDM (VSSB-OFDM)	
3.3.1	Experimental Demonstration of 340 km SSMF Transmission Using a Virtual Single Sideband OFDM Signal that Employs Carrier Suppressed and Iterative Detection Techniques	
3.3.1.1	Introduction.....	46
3.3.1.2	Concept.....	47
3.3.1.3	Equalization	49
3.3.1.4	Experimental Results.....	50
3.3.1.5	Summary.....	52
3.3.2	Experimental Demonstration of 1600 km SSMF Transmission of a Generalized Direct Detection Optical Virtual SSB-OFDM System	
3.3.2.1	Introduction.....	52
3.3.2.2	Concept.....	53
3.3.2.3	Experimental Results.....	54

3.3.2.4 Summary.....	55
References.....	56

Chapter 4

Advanced Modulation Formats

4.1 Introduction.....	79
4.2 DQPSK Generation by Using One Dual-Drive Mach-Zehnder Modulator (DD-MZM)	
4.2.1 Introduction.....	79
4.2.2 Concept.....	80
4.2.3 Experimental Setup and Results.....	82
4.2.4 Summary.....	83
4.3 Theoretical Investigations for DQPSK signal generated by one DD-MZM	
4.3.1 Introduction.....	84
4.3.2 Optical Spectra and Bit Error Rate Analysis.....	85
4.3.3 Numerical Results.....	86
4.3.4 Summary.....	88
4.4 Generation of ASK/RZ-DPSK signal by using one DD-MZM	
4.4.1 Introduction.....	88
4.4.2 Concept.....	90
4.4.3 Numerical Results.....	91
4.4.4 Summary.....	93
4.5 Quantum Limit of 4-level ASK System	
4.5.1 Introduction.....	93
4.5.2 The Optimum Level and Quantum Limit for 4ASK.....	95
4.5.3 Numerical Results.....	98

4.5.4	Summary.....	100
4.6	Improvement of Dispersion and Optical Filtering Tolerances for Quaternary Intensity Detection Using Phase Modulation and Balanced Detection Technique	
4.6.1	Introduction.....	101
4.6.2	Generation of 4ASK and PM4ASK.....	102
4.6.3	Performance Bound, Dispersion and Optical Filtering Tolerances.....	103
4.6.4	Summary.....	106
	References.....	107

Chapter 5

Optical Code Division Multiplexing

5.1	Introduction.....	130
5.2	Light Source of OCDMA	
5.2.1	Introduction.....	130
5.2.2	Concept.....	131
5.2.3	Experimental Setup and Results.....	132
5.2.4	Summary.....	134
5.3	Reducing Multiple Access Interference in an Optical Fast Frequency Hopping CDMA (OFFH-CDMA) System	
5.3.1	Introduction.....	135
5.3.2	Concept.....	137
5.3.3	Code Design and Performance Analysis.....	139
5.3.4	Numerical Results.....	145
5.3.5	Summary.....	148
5.4	Multi-Carrier CDMA	
5.4.1	Introduction.....	149

5.4.2	Concept.....	150
5.4.3	Experimental Setup and Results.....	151
5.4.4	Summary.....	152
	References.....	153

Chapter 6

Conclusions and Future Work

6.1	Conclusions.....	169
6.2	Future Work.....	170
	References.....	173

List of Publications	174
-----------------------------------	-----



List of Figures

Chapter 2

- Fig. 2.1** OFDM fundamentals: transmitter and receiver.....21
- Fig. 2.2** (a) The transmitter and (b) receiver in a Coherent Optical OFDM (CO-OFDM) system.21
- Fig. 2.3** Coherent transmitter and receiver for polarization division multiplexing (PDM).22
- Fig. 2.4** Various proposed direct detection OFDM: (a) using Hermitian symmetry and an optical filter; (b) using up-conversion and an optical filter, (c) using a frequency domain Hilbert transform. For all the three types of OFDM formats, only one photodiode is needed at the receiver.....23
- Fig. 2.5** Optical DPSK: (a) transmitter and (b) receiver.....24
- Fig. 2.6** Optical DQPSK: (a) transmitter and (b) receiver. The purpose of the two sets of optical delay interferometers is to feed the data into a simple binary decision circuit.....25
- Fig. 2.7** Optical ASK/DPSK: (a) transmitter and (b) receiver.....26
- Fig. 2.8** Optical four level ASK (4ASK): transmitter and receiver.....26
- Fig. 2.9** Optical CDMA: (a) direct sequence (DS-CDMA) and (b) fast frequency hopping (FFH-CDMA), (c) spectra encoding CDMA (SE-CDMA).....27

Chapter 3

- Fig. 3.1** Operation principles for (a) the conventional power-modulated SSB-OFDM, and (b) the proposed RF-tone assisted OFDM-A (gapped) and OFDM-B (interleaved).....59
- Fig. 3.2** Experimental setup of the RF-tone assisted OFDM.59

Fig. 3.3	Experimental results of error vector magnitude versus the carrier to signal power ratio.....	60
Fig. 3.4	Experimental results of error vector magnitude versus the input power per span.....	60
Fig. 3.5	Experimental results of BER versus OSNR. The OSA resolution is 0.2 nm.....	61
Fig. 3.6	Simulation of the error vector magnitude as a function of the chromatic dispersion.....	61
Fig. 3.7	(a) The MZM imbalance and bias deviation, and the corresponding output spectrum of the RF-tone assisted OFDM and (b) the interfered signals after photodiode and the proposed 2x2 equalization matrix compensating the imbalance effects.	62
Fig. 3.8	Experimental setup of the joint equalization technique for MZM imbalances and fiber CD.	63
Fig. 3.9	Measured RF spectra after PD, (a) ideal operation, (b) with a amplitude imbalance of $\alpha = 1.38$, (c) with a phase deviation of 0.1π , (d) with a bias deviation of $\Delta V / V_{rms}$, where V_{rms} is the root-mean square of the input signal, (e) with a time misalignment of $T_d = 10$ ps.	64
Fig. 3.10	EVM versus amplitude imbalance, (b) EVM versus phase deviation, (c) EVM versus bias deviation, where V_{rms} is the root-mean square of the input signal, (d) EVM versus the time misalignment.....	65
Fig. 3.11	Bit error rate (BER) versus the optical signal to noise ratio (OSNR) for without and without I/Q compensation scheme, before and after 800 km uncompensated transmission. Note that there is no I/Q imbalance for this plot.....	65
Fig. 3.12	Required OSNR (0.1 nm) for $BER = 10^{-3}$ versus the fiber distance with MZM imbalance.....	66

Fig. 3.13	Concept of wavelength conversion using SFG/DFG in a PPLN waveguide.....	66
Fig. 3.14	Experimental setup of OFDM wavelength conversion. The constellation and RF spectra of 8 & 16-QAM are inserted.	67
Fig. 3.15	Optical spectra after wavelength conversion. QPM: quasi-phase matching wavelength.....	67
Fig. 3.16	BER performance of the 10 Gb/s RF-tone assisted OFDM signal for both back to back and after conversion.....	68
Fig. 3.17	BER performance of 8-QAM and 16-QAM for both back to back (bb) and after wavelength conversion.....	68
Fig. 3.18	BER with different subcarrier numbers.....	69
Fig. 3.19	The progress of the power spectra of the SSB-OFDM signal and the ASE noise before and after the photodiode.....	69
Fig. 3.20	Simulated electrical power spectra of the OFDM signal.....	70
Fig. 3.21	BER versus OSNR with different optical filter bandwidth (OBW). The data rate is 10 Gbps with 4-QAM. The OFDM bandwidth is ~11.8 GHz. The Q-factor is extracted from all the received constellation point.....	70
Fig. 3.22	BER versus OSNR with different OFDM QAM formats. The optimum optical bandwidths for 4-, 16- and 64-QAM 10-Gbps SSB-OFDM signals are 13, 6.7 and 4.6 GHz.	71
Fig. 3.23	Transmitter architectures for the (a) conventional SSB-OFDM and (b) the proposed virtual SSB-OFDM. (H. T.: Hilbert Transform)	72
Fig. 3.24	Iterative detection for the virtual SSB-OFDM.....	72
Fig. 3.25	Experimental setup of the virtual SSB-OFDM.....	73
Fig. 3.26	Measured error vector magnitude (EVM) versus the receiver iteration numbers.....	73

Fig. 3.27	Measured EVM versus the carrier to signal power ratio (CSPR).....	74
Fig. 3.28	Measured bit error rate versus the optical signal to noise ratio for the conventional and the virtual SSB-OFDM. The OSA resolution is 0.2	74
Fig. 3.29	Simulated results for the conventional and the virtual SSB-OFDM. OMI (optical modulation index) is defined as $[V_{in}]_{rms}/V\pi$, where $[V_{in}]_{rms}$ is the root-mean square of the electrical input to the MZM and $V\pi$ is the switching voltage of the MZM.....	75
Fig. 3.30	The proposed generalized VSSB-OFDM (GVSSB-OFDM) with tunable gap. The optimum gap trades the signal-signal beat interference (SSBI) with the image interference.....	76
Fig. 3.31	Experimental setup for the GVSSB-OFDM system.....	76
Fig. 3.32	Measured EVM versus the frequency gap for different values of CSPR.....	77
Fig. 3.33	Measured EVM versus the carrier to signal power ratio.....	77
Fig. 3.34	Measured EVM versus the iteration number.....	78
Fig. 3.35	Measured BER versus the OSNR.	78

Chapter 4

Fig. 4.1	(a) Principle of the generation of an optical DQPSK signal with a single MZM. (b) Symbol positions and the constellation diagram.....	113
Fig. 4.2	Experimental setup.....	113
Fig. 4.3	Optical spectra of the generated NRZ, and RZ signals with different duty cycle.....	114
Fig. 4.4	Back to Back eye diagrams of the NRZ and RZ signals with different duty cycles before and after detection. The horizontal scales are all with 20 ps/div.	114
Fig. 4.5	Bit error ratio of the DQPSK signals before and after 60 km fiber transmission.....	115

Fig. 4.6	(a) DQPSK transmitter with one DD-MZM and one pulse carver, (b) DQPSK transmitter with two parallel MZMs and one pulse carver, and (c) Receiver numerical model.....	115
Fig. 4.7	(a) The optical spectra of the DQPSK signal generated by conventional two parallel MZMs. (b) The optical spectra of DQPSK signal generated by one DD-MZM.....	116
Fig. 4.8	(a) BER versus OSNR for one-MZM scheme with $T_d = 20$ ps time mismatch between the data and the pulse modulators. (b) The power penalty of the RZ formats versus the relative delay between the data and the pulse modulators.....	117
Fig. 4.9	(a) BER of the two-MZMs schemes. (b) BER of the one-MZM scheme.....	118
Fig. 4.10	The proposed scheme for ASK/ CSRZ-DPSK modulation.....	119
Fig. 4.11	System test link for the proposed ASK/RX-DPSK modulation scheme.....	119
Fig. 4.12	Back to back receiver sensitivities of label and payload versus label extinction ratio.	120
Fig. 4.13	Eye patterns of the payload before and after the low pass electrical filter, with and without the optimization scheme.....	120
Fig. 4.14	BER performances of the label in back to back and 120 km SSMF transmission.....	121
Fig. 4.15	BER performances of the payload in back to back and 120 km SSMF transmission.....	121
Fig. 4.16	The bit error rate for 4-ASK as a function of photons/bit with various M.	122
Fig. 4.17	The optimum normalized multilevel spacing and thresholds as a function of photons/ bit with (a) $M = 1$, (b) $M=10$, (c) $M=30$, (d) $M=50$. (e) The optimum normalized multilevel spacing and thresholds at a bit error rate of 10^{-9} as a	

	function of M.....	123
Fig. 4.18	Required photons/bit to achieve a bit error rate of 10^{-9} for both the binary and the quaternary formats.....	124
Fig. 4.19	Bit error rate versus the photons/bit for the RZ-4ASK format for the back to back and $CD = 510$ ps/nm with the exact and Gaussian approximation method.....	124
Fig. 4.20	The modulation and demodulation of (a) the conventional 4ASK and (b) the proposed PM4ASK formats.....	125
Fig. 4.21	(a) Bit error rates for RZ-4ASK and RZ-PM4ASK formats calculated by Monte-Carlo (MC) error counting and Karhunen-Loeve (KL) semi-analytical method. (b) BER versus SNR for both 4ASK and PM4ASK formats under the matched (QL) and optimum practical filters.....	126
Fig. 4.22	(a) Required SNR for $BER=10^{-9}$ versus residual dispersion. (b) Required SNR for $BER=10^{-9}$ versus differential group delay.....	127
Fig. 4.23	Required SNR for $BER=10^{-9}$ versus differential group delay with residual dispersion of 255 and 510 ps/ nm.....	128
Fig. 4.24	Required SNR at $BER = 10^{-9}$ versus the optical bandwidth for the conventional RZ4ASK and proposed RZ-PM4ASK formats.....	128

Chapter 5

Fig. 5.1	Experimental setup of the proposed OFFH-CDMA light source module.....	157
Fig. 5.2	Time domain waveforms at positions of A, B, and C, respectively.....	157
Fig. 5.3	(a) Optical spectrum of the FP-LD output. The inset shows the detail near the center wavelength, and (b) the time domain single pulse with a pulse-width of ~ 56.4 ps.....	158

- Fig. 5.4** (a) The output spectrum after encoding, where, $\lambda_1=1548.82$ nm, $\lambda_2=1549.9$ nm, and $\lambda_3=1550.98$ nm. (b) Encoded waveform with a bit and chip durations of 2.1 ns and 500 ps, respectively. The sequence order in time domain is $\lambda_1 \rightarrow \lambda_2 \rightarrow \lambda_3$159
- Fig. 5.5** (a) The output spectrum after encoding, where $\lambda_1=1548.82$ nm, $\lambda_2=1549.9$ nm, and $\lambda_4=1552.06$ nm. (b) Encoded signal with bit and chip durations of 2.1ns and 500ps, respectively. The sequence order in time domain is $\lambda_1 \rightarrow \lambda_2 \rightarrow \lambda_4$160
- Fig. 5.6** The transmitter and receiver for an OFFH-CDMA system with the fiber Bragg grating (FBGA) as the encoder and decoder.....161
- Fig. 5.7** (a) and (b) are a star network and the frequency allocation approach for conventional scheme. (c) and (d) are a star network and the frequency allocation approach with our proposed multi-group scheme.....161
- Fig. 5.8** The frequency slots assigned to the i -th and the j -th group. The reflected optical power by a grating is denoted as A_{ov} and the two possible partial reflected power shown in figure are denoted as $A_{|m-j|}$ and $A_{|N_R-(m-j)|}$162
- Fig. 5.9** The FBGA spectra of the 2-group codes. Note the frequency slots of different groups are overlapping.....162
- Fig. 5.10** Received signals at the i -th receiver from the j -th group. (a) Interference in the l -th transmitter from the m -th group. The used code is denoted as $F_{l,m}$ (b) Received signal of the desired transmitter, the i -th transmitter from j -th group. The used code is denoted as $F_{i,j}$. “ $b_{l,m,n}$ ” is the earlier or the present bit of the l -th transmitter from the m -th group when $n = -1$ or 0 . τ_{il} represents the relative delay chips between the two inputs.....163
- Fig. 5.11** (a) One-bit of all the 24 users are synchronously sent to the decoder of the first user to evaluate the interference, (b) to (e) correspond to group number of 1, 2, 6,

	24 for code lengths of 12, from 25 available un-overlapping frequency slots and 24 simultaneous users. The center shows the auto-correlation peaks and the side lobes are the cross-correlation interference.....	164
Fig. 5.12	The adjacent non-overlapping Gaussian apodization grating spectra. The frequency spacing is determined to allow the first nulls of adjacent gratings are coincided to increase the spectra efficiency.....	165
Fig. 5.13	(a) BER versus simultaneous users with different group numbers. The number of frequency slots q and the code weight N are equal to 25 and 12, respectively, and (b) The number of frequency slots q and the code weight N are equal to 17 and 12, respectively.....	165
Fig. 5.14	BER of systems with parameters $(q, N) = (17, 12)$ and $(q, N) = (25, 12)$	166
Fig. 5.15	Block diagram of MC-CDMA, upper part is the transmitter and lower part is the receiver.....	167
Fig. 5.16	Experimental setup of MC-CDMA.....	167
Fig. 5.17	BER curves of different number of active users and corresponding equalized constellations.....	168
Fig. 5.18	BER curves and equalized constellations for different QAM mappings.....	168

List of Tables

Table 4.1	The Optimum optical and electrical filters and the 3-dB tolerances to CD and PMD effects.....	129
------------------	---	-----

List of Acronyms

<u>Acronyms</u>	<u>Descriptions</u>
AABN	ASE-ASE Beat Noise
ADC	Analog to Digital Converter
ASE	Accumulated Spontaneous Emission
ASK	Amplitude Shift Keying
AWG	Array Waveguide Grating
BER	Bit Error Rate
BERT	Bit-Error-Ratio Tester
BPF	Band-Pass Filter
CD	Semiconductor Optical Amplifier
CDMA	Code Division Multiple Access
CDR	Clock and Data Recovery
CO-OFDM	Coherent Optical OFDM
CSPR	Carrier to Signal Power Ratio
CW	Continuous Wave
DAC	Digital to Analog Converter
DCF	Dispersion Compensating Fiber
DCM	Dispersion Compensating Module
DD-MZM	Dual Drive MZM
DFB-LD	Distributed Feedback Laser Diode
DFG	Difference Frequency Generation
DPSK	Differential Phase Shift Keying
DQPSK	Differential Quadrature Phase Shift Keying
DSC	Digital Self-Coherent

DS-CDMA	Direct Sequence CDMA
DSP	Digital Signal Processing
EDFA	Erbium-Doped Fiber Amplifier
EOM	Electric Optical Modulator
ER	Extinction Ratio
EVM	Error Vector Magnitude
FBG	Fiber Bragg Grating
FBGA	Fiber Bragg Grating Array
FDL	Fiber Delay Line
FEC	Forward Error Correction
FFH-CDMA	Fast Frequency Hopping CDMA
FFT	Fast Fourier Transform
FP-LD	Fabry-Pérot Laser Diode
FWM	Four Wave Mixing
GVSSB-OFDM	Generalized Virtual Single Sideband OFDM
IFFT	Inverse FFT
KLSE	Karhunen-Loeve Series Expansion
LAN	Local Access Network
LO	Local Oscillator
MAI	Multiple Access Interference
MAN	Metropolitan Area Network
MC-CDMA	Multi-Carrier CDMA
MGF	Moment Generating Function
MLSE	Maximum Likelihood Sequence Estimation
MZM	Mach-Zehnder Modulator
NRZ	Non-Return to Zero

OBW	Optical Filter Bandwidth
OC	Optical Circulator
OCDMA	Optical CDMA
ODI	Optical Delay Interferometer
OFDM	Orthogonal Frequency Division Multiplexing
OMI	Optical Modulation Index
ONU	Optical Network Unit
OOK	On Off Keying
OSA	Optical Spectrum Analyzer
OSNR	Optical Signal to Noise Ratio
PBS	Polarization Beam Splitter
PC	Polarization Controller
PDM	Polarization Division Multiplexing
PMD	Electro-Absorber Modulator
PON	Passive Optical Network
PPLN	Periodically Poled Lithium Niobate
PRBS	Pseudo Random Binary Sequence
PSD	Power Spectra Density
QAM	Quadrature Amplitude Modulation
QPM	Quasi-Phase Matching
ROF	Radio over Fiber
RZ	Return to Zero
SABN	Signal-ASE Beat Noise
SC	Super Continuum
SCM	Subcarrier Multiplexing
SE-CDMA	Spectra Encoding CDMA

SFG	Sum Frequency Generation
SMSR	Side Mode Suppression Ratio
SPM	Self-Phase Modulation
SSBI	Signal-Signal Beat Interference
SSFBG	Super-Structured Fiber Bragg Grating
SSMF	Standard Single Mode Fiber
TDM	Time Division Multiplexing
VOA	Variable Optical Attenuator
VSSB-OFDM	Virtual Single Sideband OFDM
WDM	Wavelength Division Multiplexing
WH	Walsh-Hadamard
XPM	Cross Phase Modulation

